FISSION GAS BEHAVIOR OF U_3Si_2 IN LWRS: EXPERIMENTAL AND COMPUTATIONAL STUDY

Y. MIAO, K. MO, Z. MEI, B. YE, S. ZHU, A.M. YACOUT
Argonne National Laboratory
9700 S Cass Ave, Lemont, IL 60439 – United States

J. HARP, K. GAMBLE
Idaho National Laboratory
2525 Fremont Ave, Idaho Falls, ID 83402 – United States

D. ANDERSSON
Los Alamos National Laboratory
Los Alamos National Laboratory, Los Alamos, NM 87546 – United States

ABSTRACT

A rate theory model was developed and parameterized for U_3Si_2 use under light water reactors (LWRs) conditions, based on both first-principle calculations and post-irradiation examinations (PIEs) data. As limited in-pile PIE data are available for U_3Si_2 at LWR temperatures, high-energy Xe ion implantation was performed to support model development. PIEs of Xe-implanted U_3Si_2 specimens unveils quantitative fission gas bubble morphology data at different temperatures, which were then utilized for optimization and validation of the model parameters. The optimized rate theory model was used to predict the fission gas behavior of U_3Si_2 under steady state LWR conditions. During steady-state operation, intragranular bubbles with bimodal size distribution dominate U_3Si_2's fission gas behavior in LWRs, leading to controllable gaseous swelling. The model optimized in this study can also be used to predict the fission gas behavior during a loss-of-coolant accident to help better understand the accident tolerance of U_3Si_2 in LWRs.

1. Introduction

Developing a novel fuel-cladding solution with enhanced accident tolerance has become a focus of the nuclear energy community since the severe nuclear accident in Fukushima [1]. With advantageous heavy metal density and thermos-physical properties, U_3Si_2 is regarded as a promising accident tolerant fuel (ATF) candidate for light water reactors (LWRs) and thus has been intensely studied and invested in over the past few years. To evaluate the feasibility of using U_3Si_2 as a LWR fuel, its fuel performance must be well understood and accurately predicted. A series of computational and experimental efforts have been made to investigate U_3Si_2's fuel behavior under LWR conditions [2-6], including the development of a rate theory model that is capable of predicting U_3Si_2's fission gas behavior during steady state operation [7]. However, due to the absence of in-pile irradiation data collected at LWR temperatures, the fuel performance modeling of U_3Si_2 as a LWR ATF has to rely on post-irradiation examination (PIE) data from low-temperature (<250ºC) research reactor data [8]

and atomistic simulation results. Experimental results obtained under LWR conditions are required to optimize, verify, and validate these models.

In nuclear fuels, the majority of radiation-induced microstructural modifications are caused by fission fragments, which are ~100 MeV energetic heavy ions. Therefore, high-energy heavy ion irradiation generated by accelerators is able to replicate the radiation effects in nuclear fuels [9-12]. Therefore, before the detailed microstructural PIE data from ATF-1 in-pile irradiation campaign is available, high-energy ion irradiation can be adopted to provide some preliminary but essential experimental references on U_3Si_2's microstructural responses to irradiation so as to support the fuel performance model development that is required for the fuel qualification of U_3Si_2.

In this study, U_3Si_2 specimens were implanted by high-energy Xe ions at LWR temperatures in Argonne Tandem Linac Accelerator System (ATLAS). The morphology of Xe bubbles formed under different implantation conditions were quantitatively investigated by transmission electron microscopy (TEM) techniques. These PIE data of Xe bubbles were then utilized to optimize and validate a rate theory developed solely based on research reactor experiments and density functional theory (DFT) calculations [7]. The fission gas behavior predicted by the improved code was compared with both previous simulation results as well as experimental observations.

2. Methods

2.1 Ion Irradiation and Post-Irradiation Examinations (PIEs)

The U_3Si_2 specimens (Φ8.3 mm × 2 mm discs) used in this ion irradiation experiment were sectioned from U_3Si_2 pellets that were fabricated using the same procedures as those pellets irradiated in the Advanced Test Reactor (ATR) as a part of the ATF-1 irradiation campaign [13]. The specimen surface was mechanically polished to 0.05 μm before final vibratory polishing. Three specimens were then implanted by a 100 particle nA 84 MeV Xe ion beam in the ATLAS facility at 300ºC, 450ºC, and 600ºC, respectively. 84 MeV Xe ions create ~8 μm deep radiation damage and Xe deposition profiles in the U_3Si_2 specimens according to the SRIM calculation following Stollller et al's method [14]. Assuming a 2D Gaussian beam profile, a uniform peak ion fluence of 1.39×10^{17} ions/cm^2 was applied for all three specimens, which corresponds to a ~499 dpa peak radiation dose and a ~0.92% peak Xe concentration. The PIE of these Xe implanted specimens was conducted at the Materials Characterization Suite (MaCS) in Center for Advanced Energy Studies (CAES). TEM lamellae were prepared from these Xe implanted specimens using an FEI Quanta 3D FEG focused ion beam (FIB) system. The lamellae were then characterized using an FEI Tecnai TF30-FEG STwin STEM working at 300 kV. Both high-angle annular dark field (HAADF) Z-contrast and bright field (BF) diffraction contrast imaging techniques were used to examine the bubble morphology in the TEM lamellae. It is worth mentioning that the as-fabricated U_3Si_2 contains ~15 vol.% USi and UO_2 inclusions. The PIEs of the ion irradiated samples were focused on the U_3Si_2 matrix.

2.2 Rate Theory Model for U_3Si_2 under LWR conditions

The GRASS-SST fission gas behavior code, which is based on a mechanistic rate theory model governing the evolution of fission gas bubbles of different sizes at different locations in monolithic polycrystalline fuels, was used in this study [15]. Previously, using research reactor PIE data and first principle calculations, the GRASS-SST rate theory model was parameterized for U_3Si_2 in LWRs and was utilized to study U_3Si_2's fission gas behavior under steady state LWR conditions [7].

In this study, the fission bubble morphology data collected from PIEs of Xe implanted specimens were adopted to validate and optimize the rate theory model. For the rate theory model in the GRASS-SST code, the major difference between in-pile neutron irradiation and ion irradiation is the correlation between Xe generation/accumulation rate and radiation damage rate. During in-pile neutron irradiation, each fission reaction produces two fission products. Although only ~0.24 of the two products generated in each fission reaction are Xe ions, all the fission products contribute to the radiation damage and consequent radiation enhanced diffusion (RED). On the contrary, in Xe ion irradiation experiments, radiation damage and RED is solely induced by Xe ions. In the GRASS-SST rate theory model, both Xe generation rate and RED are calculated by multiplying fission density rate and a respective coefficient. Hence, the coefficient used to calculate RED effect was modified for ion irradiation so that the unique correlation between Xe accumulation rate and radiation damage rate in the ion implantation experiments can be captured. With the modified rate theory model, the bubble morphology in Xe implanted specimens can be compared with the model's predictions. Thus, the reliability of the rate theory model was further improved.

3. Results and Discussion

3.1 Bubble Morphology at Various LWR Temperatures

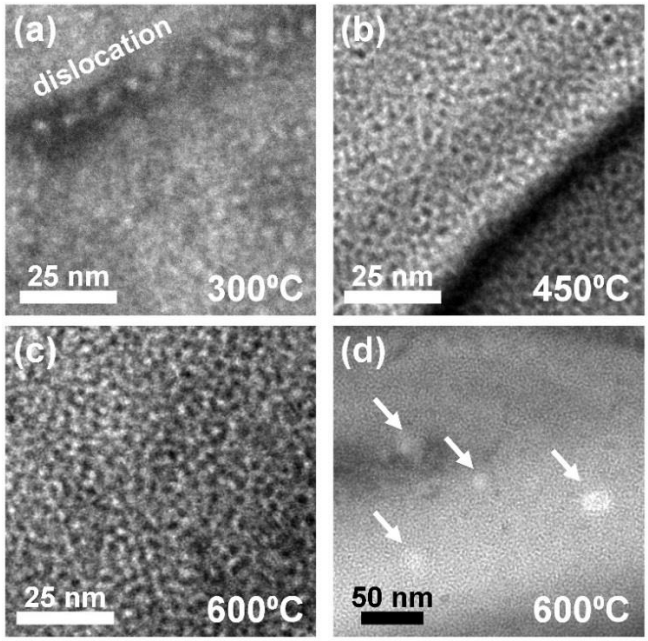

Fig 1. Morphology of intragranular Xe bubbles shown by defocused TEM bright-field images: (a) small lattice and dislocation intragranular bubbles formed at 300ºC; (b) small lattice intragranular bubbles formed at 450ºC; (c) small lattice intragranular bubbles formed at 600ºC; (d) large lattice intragranular bubbles formed at 600ºC

When irradiated, U_3Si_2 has been reported to oxidize even in a TEM chamber [6], where only a tracing amount of oxygen/moisture exists. In this study, the vacuum level of the ion irradiation chamber was approximately 10^{-4} Pa, which is slightly higher than the typical TEM vacuum (~10^{-5} Pa). As a result, oxidation layers formed in all three specimens after irradiation. A prominent temperature effect on oxidation was observed: the thickness of the oxidation layer increase from ~1 μm at 300ºC to ~4 μm at 600ºC. The oxidation layer is U-enriched and Si-depleted according to energy dispersive X-ray spectroscopy (EDS),

whereas the Si was found to diffuse inward and form a Si-enriched USi_{2-x} layer between the oxidation layer and remainder of U_3Si_2. As the range of 84 MeV Xe ions in U_3Si_2 is much deeper than 4 μm, U_3Si_2 phase was preserved in all of the three samples near the Xe deposition peak at approximately 6.5 μm from the surface. Thus, the Xe bubbles can be investigated in U_3Si_2 implanted at all three representative LWR temperatures examined in this study.

Intragranular bubbles formed in U_3Si_2 lattice of all three specimens implanted at different temperatures. At 300ºC, spherical lattice intragranular bubbles were observed around the region corresponding to the peak of Xe deposition predicted by SRIM. As the implantation temperature is elevated to 450ºC, the spherical shape and size of these lattice intragranular bubbles remain. However, once the implantation temperature is as high as 600ºC, a prominent bubble morphology change occurs. In addition to these spherical and small bubbles, faceting bubbles with tens of nm in size also formed in U_3Si_2 lattice. Bubble morphology investigations clearly show that lattice intragranular bubbles have a monomodal size distribution with an average size of ~2.7 nm at 300ºC and 450ºC. At 600ºC, lattice intragranular bubbles have a bimodal size distribution. Aside from these small spherical bubbles similar to those observed at lower LWR temperatures, large faceting bubbles of ~20 nm in size coexist within the U_3Si_2 grains, resulting a bimodal size distribution. This implies the activation of bubble coalescence occurs between 450ºC and 600ºC.

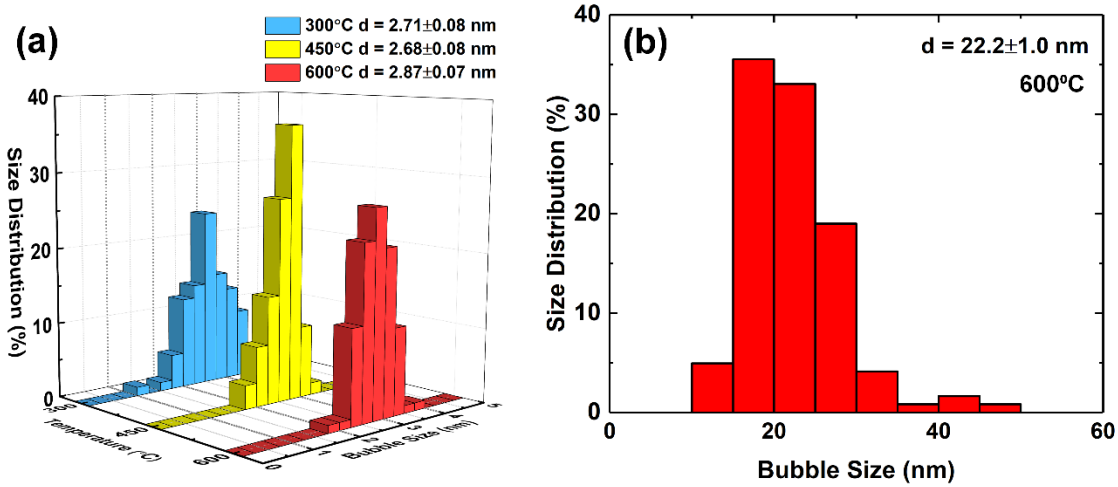

Fig 2. Size distribution of intragranular Xe bubbles: (a) small intragranular bubbles formed at various implantation temperatures; (b) large intragranular bubbles formed at 600ºC

The U_3Si_2 specimens investigated in this study contain few dislocations prior to Xe implantation [6]. After implantation at 300ºC, a prominent dislocation accumulation induced by irradiation was observed. Some of the radiation-induced dislocations are localized to form dislocation arrays, which are also known as low-angle grain boundaries (LAGBs). Both separate dislocations and LAGBs are decorated by Xe bubbles that are larger than lattice intragranular bubbles. At higher implantation temperatures, radiation-induced dislocations were hardly distinguished in the specimens, which indicated that the annealing effect suppressed the defect accumulation. As a result, dislocation bubbles play a marginal role at these temperatures.

Additionally, in the specimen implanted at 300ºC, bubbles were found to accumulate on the high-angle grain boundaries (HAGBs), as shown in Fig. 3(a). The size distribution of these

interagranular bubbles were found to slightly vary with type of grain boundaries. The bubble size ranges from 1.5 nm up to 9.5 nm with an average size around 4.22 nm, which is larger than that of the lattice intragranular bubbles but is comparable to that of the dislocation intragranular bubbles.

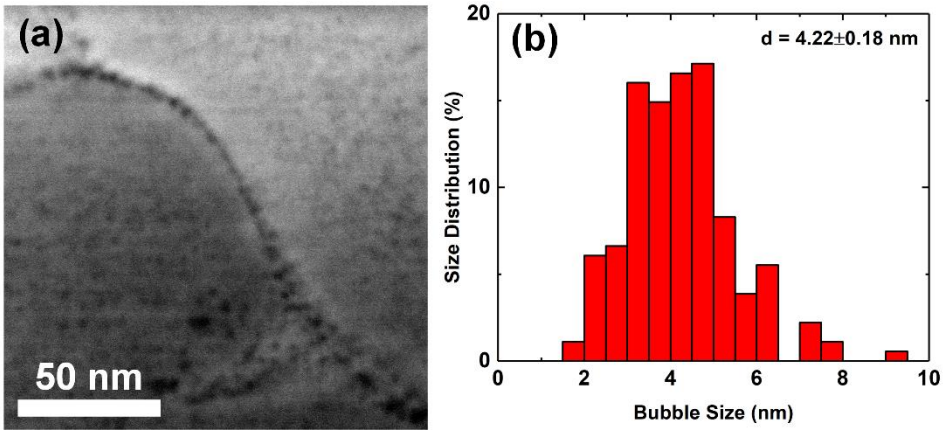

Fig 3. Interagranular bubbles on a HAGB in the U_3Si_2 specimen implanted at 300ºC: (a) a STEM HAADF Image; (b) size distribution

At higher implantation temperatures, namely 450ºC and 600ºC, intergranular bubbles are expected to further evolve due to faster diffusion of Xe in U_3Si_2. Unfortunately, there are only a few preexisting grain boundaries in the TEM lamellae prepared from these two specimens; and preferential oxidation near grain boundaries at elevated irradiation temperatures made it infeasible to characterize intergranular bubbles at 450ºC and 600ºC. Further efforts including surface protection coating will be made to suppress the radiation-enhanced oxidation of U_3Si_2 in the irradiation chamber to enable the study of intergranular bubble morphology beyond ~450ºC.

3.2 Optimization and Validation of the Rate Theory Model

As previously reported, the rate theory model of the GRASS-SST code has been modified and parameterized using a combination of research reactor experimental data and DFT calculation results [7]. The research reactor and DFT data provided limited information to the behavior of Xe on the grain boundaries. In this study, the quantitative morphology of intergranular Xe bubbles collected at 300ºC was utilized to optimize one of the most important grain boundary related parameters, χ (see Table. 1).

Table 1: The rate theory model parameters after optimization

Symbol	Parameter	Value	Origin
D_0	intrinsic Xe diffusivity (pre-exponential constant)	7.73×10^{-7} m^2/s	D
Q	intrinsic Xe diffusivity (activation energy)	1.68 eV	D
D_g^{RED}	Xe radiation-enhanced diffusivity (RED) factor	4.0×10^{-16} m^5	I
f_n	bubble nucleation factor	0.01	R
b_0	bubble resolution factor	1.0×10^{-25} m^3	R
γ	surface energy of U_3Si_2	1.32 J/m^2	D
gbr(1)	effective resolution factor of Xe from grain faces	1.00	R
χ	enhancement factor of Xe RED on grain boundaries	14	I

Origin: D: DFT calculation; I: ion irradiation experiments (this work); R: research reactor data.

In addition, the radiation enhanced diffusivity of Xe in U_3Si_2 cannot be calculated as straightforward as intrinsic (thermally-activated) Xe diffusivity. Hence, D_g^{RED} was also optimized using the ion irradiation experimental results. These two key rate theory parameters were determined by fitting the bubble size distribution and number density observed in the Xe implantation experiment. The key rate theory parameters after optimization are listed in Table.1

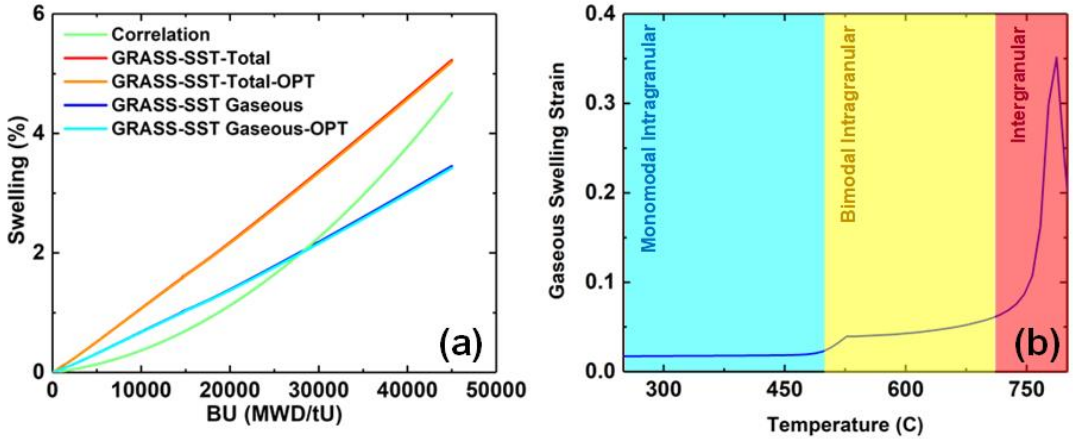

Fig 4. Optimization and validation of the rate theory model: (a) comparison of the swelling strain values predicted by the original BISON correlation and the rate theory model before and after optimization; (b) three temperature regimes of gaseous swelling in U_3Si_2 predicted by optimized rate theory model

The updated model was then used to predict the fission gas behavior under typical steady state LWR conditions by adopting the operation parameters predicted by a BISON study [2]. As intragranular bubbles dominate the fission gas behavior during normal operation, the rate theory models before and after optimization yield very similar swelling results (see Fig. 4(a)). More importantly, during the ion irradiation, the heating effect of the ion beam creates a ~20 K/mm temperature gradient in the U_3Si_2 specimens. At that temperature gradient, the optimized rate theory model predicts a gas swelling strain vs. temperature profile as illustrated in Fig. 4(b). Similar to what was reported in Ref. [7], three temperature regimes, the gas behavior of which is respectively dominated by intragranular bubbles with monomodal size distribution, intragranular bubbles with bimodal size distribution, and intergranular bubbles, can be identified. The transition between monomodal and bimodal intragranular bubble regimes occurs at approximately 480ºC, which is consistent with the observation of this study. Hence, ion implantation experiments reported in this study also validate the reliability of the rate theory model. The rate theory model developed in this study have also been used to predict fission gas behavior of U_3Si_2 under accident scenarios after adopting models governing bubble evolution kinetics during power transients [16].

4. Conclusion

In this study, a systematic high-energy Xe implantation experiment was performed at elevated temperatures to provide direct experimental data on fission gas behavior of U_3Si_2 in LWRs. The microstructure characterization of the implanted specimens produced quantitative morphology data of Xe bubbles. A rate theory model of fission gas behavior that was previously developed for U_3Si_2 in LWRs was further improved and validated using the ion implantation experiment results. The model is capable of reliably predicting the fission

gas behavior under both steady-state and transient LWR conditions. High-energy ion irradiation proved to be a powerful and economical tool to provide direct experimental observations of novel nuclear fuels' fuel performance to support modeling development and predict its in-pile behavior.

5. Acknowledgements

This work was funded by the Accident Tolerant Fuel High-Impact Problems (ATF-HIP) of the U.S. Department of Energy (DOE)'s Nuclear Energy Advanced Modeling and Simulation (NEAMS) program. The submitted manuscript has been authored by a contractor of the U.S. Government under Contract DEAC07-05ID14517. Accordingly, the U.S. Government retains a non-exclusive, royalty free license to publish or reproduce the published form of this contribution, or allow others to do so, for U.S. Government purposes. Los Alamos National Laboratory, an affirmative action/equal opportunity employer, is operated by Los Alamos National Security, LLC, for the National Nuclear Security Administration of the U.S. Department of Energy under Contract No. DE-AC52-06NA25396.

The authors would also like to acknowledge the help of Matthew Hendricks on the ATLAS irradiation. This research used resources of Argonne National Laboratory's ATLAS facility, which is a DOE Office of Science User Facility. The efforts involving Argonne National Laboratory were sponsored under Contract no. DE-AC02-06CH11357 between UChicago Argonne, LLC and the U.S. Department of Energy. This work was supported by the U.S. Department of Energy, Office of Nuclear Energy under DOE Idaho Operations Office Contract DE-AC07-051D14517 as part of a Nuclear Science User Facilities experiment. The isotope(s) used in this research were supplied by the United States Department of Energy Office of Science by the Isotope Program in the Office of Nuclear Physics.

Fabrication of the samples used in this work was supported by the U.S. Department of Energy, Office of Nuclear Energy. Fabrication was part of a collaboration led by Westinghouse Electric Company comprising several national laboratories, vendors, and universities awarded in response to the DE-FOA-0001063 funding opportunity. The authors would like to acknowledge the assistance of the support staff associated with the Fuels Applied Science Building at Idaho National Laboratory specifically Rita Hoggan for preparing samples for ion irradiation.

6. References

[1] Zinkle, S. J., Terrani, K. A., Gehin, J. C., Ott, L. J., & Snead, L. L. (2014). Accident tolerant fuels for LWRs: A perspective. *Journal of Nuclear Materials*, *448*(1-3), 374-379.

[2] Metzger, K. E., Knight, T. W., & Williamson, R. L. (2014). *Model of U3Si2 fuel system using BISON fuel code* (No. INL/CON-13-30445). Idaho National Laboratory (INL).

[3] White, J. T., Nelson, A. T., Dunwoody, J. T., Byler, D. D., Safarik, D. J., & McClellan, K. J. (2015). Thermophysical properties of U3Si2 to 1773K. *Journal of Nuclear materials*, *464*, 275-280.

[4] Middleburgh, S. C., Grimes, R. W., Lahoda, E. J., Stanek, C. R., & Andersson, D. A. (2016). Non-stoichiometry in U 3 Si 2. *Journal of Nuclear Materials*, *482*, 300-305.

[5] Yao, T., Gong, B., He, L., Harp, J., Tonks, M., & Lian, J. (2018). Radiation-induced grain subdivision and bubble formation in U3Si2 at LWR temperature. *Journal of Nuclear Materials*, *498*, 169-175.

[6] Miao, Y., Harp, J., Mo, K., Bhattacharya, S., Baldo, P., & Yacout, A. M. (2017). Short Communication on "In-situ TEM ion irradiation investigations on U 3 Si 2 at LWR temperatures". *Journal of Nuclear Materials*, *484*, 168-173.

[7] Miao, Y., Gamble, K. A., Andersson, D., Ye, B., Mei, Z. G., Hofman, G., & Yacout, A. M. (2017). Gaseous swelling of U3Si2 during steady-state LWR operation: A rate theory investigation. *Nuclear Engineering and Design*, *322*, 336-344.
[8] Kim, Y. S., Hofman, G. L., Rest, J., & Robinson, A. B. (2009). Temperature and dose dependence of fission-gas-bubble swelling in U3Si2. *Journal of Nuclear Materials*, *389*(3), 443-449.
[9] Pellin, M. J., Yacout, A. M., Mo, K., Almer, J., Bhattacharya, S., Mohamed, W., ... & Zhu, S. (2016). MeV per nucleon ion irradiation of nuclear materials with high energy synchrotron X-ray characterization. *Journal of Nuclear Materials*, *471*, 266-271.
[10] Ye, B., Bhattacharya, S., Mo, K., Yun, D., Mohamed, W., Pellin, M., ... & Wiencek, T. (2015). Irradiation behavior study of U–Mo/Al dispersion fuel with high energy Xe. *Journal of Nuclear Materials*, *464*, 236-244.
[11] Ye, B., Jamison, L., Miao, Y., Bhattacharya, S., Hofman, G. L., & Yacout, A. M. (2017). Cross section TEM characterization of high-energy-Xe-irradiated U-Mo. *Journal of Nuclear Materials*, *488*, 134-142.
[12] Miao, Y., Yao, T., Lian, J., Zhu, S., Bhattacharya, S., Oaks, A., ... & Mo, K. (2018). Nano-crystallization induced by high-energy heavy ion irradiation in UO 2. *Scripta Materialia*, in press.
[13] Harp, J. M., Lessing, P. A., & Hoggan, R. E. (2015). Uranium silicide pellet fabrication by powder metallurgy for accident tolerant fuel evaluation and irradiation. *Journal of Nuclear Materials*, *466*, 728-738.
[14] Stoller, R. E., Toloczko, M. B., Was, G. S., Certain, A. G., Dwaraknath, S., & Garner, F. A. (2013). On the use of SRIM for computing radiation damage exposure. *Nuclear instruments and methods in physics research section B: beam interactions with materials and atoms*, *310*, 75-80.
[15] Rest, J. (1978). *GRASS-SST: a comprehensive, mechanistic model for the prediction of fission-gas behavior in UO 2-base fuels during steady-state and transient conditions* (No. NUREG/CR--0202). Argonne National Laboratory.
[16] Miao, Y., Gamble, K. A., Andersson, D., Mei, Z. G., & Yacout, A. M. (2018). Rate theory scenarios study on fission gas behavior of U 3 Si 2 under LOCA conditions in LWRs. *Nuclear Engineering and Design*, *326*, 371-382.